ICSV14
Cairns • Australia
9-12 July, 2007

EIGENFREQUENCY COMPUTATION BY THE FINITE SINE TRANSFORM METHOD ON A RECTANGULAR PLATE CARRYING ARBITRARY NUMBER OF CONCENTRATED MASSES AND SPRINGS

Yin Zhang

State Key Laboratory of Nonlinear Mechanics (LNM), Institute of Mechanics, Chinese Academy of Sciences, Beijing 100080, People's Republic of China
zhangyin@lnm.imech.ac.cn

Abstract

A generalized finite sine transform method (FSTM) is presented in this paper and applied to the eigenfrequency computation of a rectangular plate with arbitrarily distributed concentrated masses and translational springs. Compared with the analytical-and-numerical combined method (ANCM), FSTM keeps the same number of mode shapes in the system eigenfrequencies computation in order to have the convergence. However, unlike ANCM or the finite element method (FEM), whose eigenfrequency computation depends on the number of mode or element. The eigenfrequency computation by FSTM is mainly dependent on the total number of concentrated masses and springs. Therefore, the FSTM computation on the system eigenfrequencies is much faster when the total number of concentrated masses and springs is small.

NOMENCLATURE

E, υ :Young's modulus and Poisson's ratio of the plate.

a, b, h : Plate length, width and thickness, respectively.

M , D : Mass per unit area of the plate and plate flexural rigidity, $D = \dfrac{Eh^3}{12(1-\upsilon^2)}$.

K_i, M_i : Concentrated spring stiffness and mass, respectively.

a_i, b_i : Concentrated translational spring coordinates.

u_i, v_i : Concentrated mass coordinates.

∇^4 : Operator defined as $\nabla^4 = \dfrac{\partial^4}{\partial x^4} + 2\dfrac{\partial^4}{\partial x^2 \partial y^4} + \dfrac{\partial^4}{\partial y^4}$

W, ω : Plate transverse displacement and eigenfrequency, respectively.

1. INTRODUCTION

When a mass is added to a structure, it results in the shift of the system resonant frequencies, traveling wave propagation and damping etc [1, 2]. Those shifting properties have been utilized as the mechanisms for the development of various mass sensing sensors [1-8]. With the coating design which can specify the certain chemical vapor deposition distribution on the resonator, the chemical components of vapor adsorbed can be analyzed with this mass sensing resonator [2, 7, 8]. Or with the information on the deposition layer distribution, the added mass to the accuracy of attogram scale can be determined [5, 6]. Clearly, the amount of the adsorbed mass and its location on the resonator structures are the only two factors determining the system resonant frequency shift if the mass is modeled as concentrated mass [3, 9-15]. Compared with the whole resonator, the size of adsorbed mass is very small in many nanoelectromechanical (NEMS) mass sensing applications [3, 6]; therefore, the concentrated mass model is applied. Recent experiment of an *E.Coli* bacteria adsorption on a mass resonator by Ramos *et al.*[16] shows a surprising 24% eigenfrequency increase instead of decrease. Because adding inertia mass can only decrease the system eigenfrequency, Ramos *et al.*[16] argue that the adsorption of the bacteria also increases the system rigidity and this rigidity increase surpasses the increase of inertia mass, which results in the increase of the system eigenfrequency. Incorporating the concentrated translational spring in the model in essence plays the role of increasing the system rigidity.

Among the literatures [9-15], two major methods of modeling the plate with concentrated masses/springs can be roughly categorized. The first one is to treat concentrated masses/springs as constraints [9, 10, 11]. In the constraint method, the concentrated masses/springs do not appear in the governing equation explicitly. Instead, it is that inertial forces which can be related to the concentrated masses/springs appear in the governing equation and the problem is solved by using the displacement constraint condition [9, 10] or by using the Green's function of a constrained system [11]. As shown in those three papers [9, 10, 11], the constraint approach is rather complex and lengthy in both modeling and solution. The second method is to use Dirac delta function to incorporate the concentrated masses/springs in the governing equation [12, 13, 14]. Amba-Rao [12] develops the finite sine transform method (FSTM) for the plate with four edges simply-supported. Magrab [13] extends Amba-Rao's FSTM to the Levy plates by using Laplace transform. Shah and Datta14] incorporate the effect of moment of inertia of the concentrated mass. Chiba and Sugimoto [15] equivalently use Dirac delta function to model the effects of the concentrated spring and mass for a cantilever plate. As the concentrated mass/spring can severely distort the mode shapes of a uniform plate and shift its eigenfrequencies, the eigenfrequency computation of the plate carrying concentrated masses/springs requires a large number of elements or modes to converge. In Wu and Luo's computation example [10], the eigenfrequency computation is to solve the eigenvalue problem of an 175×175 matrix (FEM) or a 30×30 matrix (ANCM). The eigenfrequency computation by Chiba and Sugimoto's [15] is an eigenvalue problem of a 50×50 matrix. Obviously, such computation is very expensive for the mass sensing sensor or the sensor array which consists of hundreds or thousands of micro-sensors. As pointed out by Wu and Luo [10] and also to author's best knowledge, FSTM so far is only applied to the simple case of single one concentrated mass [12, 13, 14]. In this paper, the generalized FSTM on the eigenfrequency computation of the rectangular plate carrying arbitrary number of concentrated masses and springs is presented. The eigenfrequencies obtained by the generalized FSTM are also compared with those of FEM and ANCM.

2. GOVERNING EQUATIONS AND FSTM

The governing equation of a rectangular plate with *single one* concentrated mass is given by Amba-Rao [12], Magrab [13], Shah and Datta [14]. In all of these three papers [12, 13, 14], the presence of the concentrated mass is modeled by the Dirac delta function. Shah and Datta's model [14] considers the effect of moment of inertia of the concentrated mass. For the sake of brevity, the governing equation for a rectangular plate with arbitrarily distributed masses and translational springs is directly given as follows

$$D\nabla^4 W + [M + \sum_{i=1}^{r} M_i \delta(x-u_i)\delta(y-v_i)]W_{tt} + \sum_{i=1}^{s} K_i \delta(x-a_i)\delta(y-b_i)]W = 0 \qquad (1)$$

Here $W_{tt} = \frac{\partial^2 W}{\partial t^2}$. δ is the Dirac delta function. There are *r* concentrated masses and *s* concentrated translational springs. The plate is assumed isotropic and homogeneous. The equation above does not include the concentrated mass effect of moment of inertia.
The plate transverse displacement *W* is assumed to have the following solution form

$$W = \psi(x,y)e^{i\omega t} \qquad (2)$$

Substitute equation (2) into equation (1), the following equation is obtained

$$\nabla^4 \psi - \frac{\omega^2}{D}[M + \sum_{i=1}^{r} M_i \delta(x-u_i)\delta(y-v_i)]\psi + \frac{1}{D}\sum_{i=1}^{s} K_i \delta(x-a_i)\delta(y-b_i)]\psi = 0 \qquad (3)$$

$\psi(x, y)$ is the spatial part solution of the plate with the concentrated masses / springs and assumed to have the following expression when the four edges of the plate are simply-supported [12]

$$\psi(x,y) = \frac{4}{ab}\sum_{m=1}^{\infty}\sum_{n=1}^{\infty}\Omega_{mn}\sin(\alpha_m x)\sin(\beta_n y) \qquad (4)$$

Equation (4) is a double Fourier expansion of $\psi(x, y)$ and Ω_{mn} is thus defined as

$$\Omega_{mn} = \int_0^a \int_0^b \psi(x,y)\sin(\alpha_m x)\sin(\beta_n y)dxdy \qquad (5)$$

$\alpha_m = \frac{m\pi}{a}$ and $\beta_n = \frac{n\pi}{b}$. $\sin(\alpha_m x)\sin(\beta_n y)$ is the $m-n$th mode shape of a uniform plate with four edges simply-supported.
Times equation (3) with $\sin(\alpha_m x)\sin(\beta_n y)$ and have a double integral operation, the following equation is derived

$$\int_0^a \int_0^b \{\nabla^4 \psi - \frac{\omega^2}{D}[M + \sum_{i=1}^{r} M_i \delta(x-u_i)\delta(y-v_i)]\psi + \frac{1}{D}\sum_{i=1}^{s} K_i \delta(x-a_i)\delta(y-b_i)]\psi\}\sin(\alpha_m x)\sin(\beta_n y)dxdy = 0 \qquad (6)$$

Substitute equation (4) into equation (6) except the terms related to the concentrated masses and springs. Via the integration by parts and using the boundary conditions, the Dirac delta function integration property and the orthogonality of the sine functions, equation (6) is now re-written as

$$\pi^4(\frac{m^2}{a^2}+\frac{n^2}{b^2})^2\Omega_{mn} - \frac{M\omega^2}{D}\Omega_{mn} - \frac{\omega^2}{D}\sum_{i=1}^{r} M_i \psi(u_i, v_i)\sin(\alpha_m u_i)\sin(\beta_n v_i) + \frac{1}{D}\sum_{i=1}^{s} K_i \psi(a_i, b_i)\sin(\alpha_m a_i)\sin(\beta_n b_i) = 0 \qquad (7)$$

From the above equation, Ω_{mn} is solved as follows

$$\Omega_{mn} = \frac{\frac{\omega^2}{D}\sum_{i=1}^{r} M_i \psi(u_i, v_i)\sin(\alpha_m u_i)\sin(\beta_n v_i) - \frac{1}{D}\sum_{i=1}^{s} K_i \psi(a_i, b_i)\sin(\alpha_m a_i)\sin(\beta_n b_i)}{\pi^4(\frac{m^2}{a^2}+\frac{n^2}{b^2})^2 - \frac{M\omega^2}{D}} \tag{8}$$

Substitute equation (8) into equation (4), $\psi(x, y)$ is now re-written as the following

$$\psi(x,y) = \sum_{i=1}^{r} A_i(\omega, x, y)\psi(u_i, v_i) - \sum_{i=1}^{s} B_i(\omega, x, y)\psi(a_i, b_i) \tag{9}$$

And

$$A_i(\omega, x, y) = \frac{4\omega^2 M_i}{abD}\sum_{m=1}^{\infty}\sum_{n=1}^{\infty} \frac{\sin(\alpha_m u_i)\sin(\beta_n v_i)\sin(\alpha_m x)\sin(\beta_n y)}{\pi^4(\frac{m^2}{a^2}+\frac{n^2}{b^2})^2 - \frac{M\omega^2}{D}},$$

$$B_i(\omega, x, y) = \frac{4K_i}{abD}\sum_{m=1}^{\infty}\sum_{n=1}^{\infty} \frac{\sin(\alpha_m a_i)\sin(\beta_n b_i)\sin(\alpha_m x)\sin(\beta_n y)}{\pi^4(\frac{m^2}{a^2}+\frac{n^2}{b^2})^2 - \frac{M\omega^2}{D}}$$

Equation (9) is valid for any x, y, so let $(x, y,) = (u_i, v_i)$ (i = 1 to r) and$(x, y,) = (a_i, b_i)$ (i = 1 to s) into equation (9) and after simple manipulation, the following equation is obtained

$$CV = 0 \tag{10}$$

C is a $(r + s) \times (r + s)$ matrix and $C = C(\omega)$. $C(\omega)$ is given as follows

$$C(\omega) = \begin{pmatrix}
A_1(\omega,u_1,v_1)-1 & A_2(\omega,u_1,v_1) & \dots & A_r(\omega,u_1,v_1) & -B_1(\omega,u_1,v_1) & \dots & -B_s(\omega,u_1,v_1) \\
A_1(\omega,u_2,v_2) & A_2(\omega,u_2,v_2)-1 & \dots & A_r(\omega,u_2,v_2) & -B_1(\omega,u_2,v_2) & \dots & -B_s(\omega,u_2,v_2) \\
\dots & \dots & \dots & \dots & \dots & \dots & \dots \\
A_1(\omega,u_r,v_r) & A_2(\omega,u_r,v_r) & \dots & A_r(\omega,u_r,v_r)-1 & -B_1(\omega,u_r,v_r) & \dots & -B_s(\omega,u_r,v_r) \\
A_1(\omega,a_1,b_1) & A_2(\omega,a_1,b_1) & \dots & A_r(\omega,a_1,b_1) & -B_1(\omega,a_1,b_1)-1 & \dots & -B_s(\omega,a_1,b_1) \\
\dots & \dots & \dots & \dots & \dots & \dots & \dots \\
A_1(\omega,a_s,b_s) & A_2(\omega,a_s,b_s) & \dots & A_r(\omega,a_s,b_s) & -B_1(\omega,a_s,b_s) & \dots & -B_s(\omega,a_s,b_s-1)
\end{pmatrix}$$

V is a $r + s$ vector and

$V^T = [\psi(u_1,v_1),\ \psi(u_2,v_2),\ \dots\ \psi(u_r,v_r),\ \psi(a_1,b_1),\ \psi(a_2,b_2),\ \dots\ \psi(a_s,b_s)]$. As far as *not all* of (u_i, v_i) and (a_i, b_i) are on the plate nodes, which mathematically means V has a nontrivial solution, the determinant of C must be zero. $|C| = 0$ is the characteristic equation to determine the eigenfrequency ω of the plate with the concentrated masses and springs.

3. COMPUTATION EXAMPLE

All the following elastic properties and dimensions of plate are taken from Wu and Luo's computation example [10] in order to have a comparison with their ANCM and FEM results. The schematic diagram of the rectangular plate with three concentrated masses and three translational springs is shown in figure 1. The parameters related to the computation are listed as follows:

a = 2.0 m, b = 3.0 m, h = 0.005 m; $E = 2.051 \times 10^{11}\ Pa$, $M = 39.25\ kg/m^2$, υ = 0.3;

M_1 = 70.0 kg, $u_1 = 0.375a$, $v_1 = 0.25b$; M_2 = 50.0 kg, $u_2 = 0.5a$, $v_2 = 0.625b$;

M_3 = 60.0 kg, $u_3 = 0.75a$, $v_3 = 0.5b$; K_1 = 106 N/m, $a_1 = 0.125a$, $b_1 = 0.25b$;

K_2 = 104 N/m, $a_2 = 0.5a$, $b_2 = 0.5b$; K_3 = 105 N/m, $a_3 = 0.625a$, $b_3 = 0.625b$.

Although in equation (4), $\psi(x, y)$ is symbolically expressed by the mode summation from $m = 1$ to ∞ and $n = 1$ to ∞, only finite number of mode can be used during the computation. Generally, the modes with the lowest eigenfrequencies should be given the priority to be used in the modal expansion of $\psi(x, y)$. For a uniform plate with four edges hinged, the natural frequency ω_{mn} is given as follows [17]

$$\omega_{mn} a^2 \sqrt{\frac{M}{D}} = \pi^2 [m^2 + n^2 (\frac{a}{b})^2] \tag{11}$$

With this formula and the plate dimensions given above, the first 9 modes with lowest frequencies for the uniform plate are 1-1, 1-2, 2-1, 1-3, 2-2, 2-3, 1-4, 3-1 and 3-2 modes (First number is m, the second is n. $m - n$ mode in this case is $\sin(m\pi x/a)\sin(n\pi y/b)$). Equation (11) gives the idea on how to take the modes with the lowest frequencies. In order to compare with Wu and Luo's ANCM results [10], m is taken from 1 to 6 and n is taken from 1 to 5. So there are total 30 modes used in the computation. The reason of taking some many modes in computation mentioned in introduction part is that the concentrated mass/spring can severely distort the mode shapes of a uniform plate and the large mode number is required for the convergence. FSTM also shows very good convergence when mode number increases.

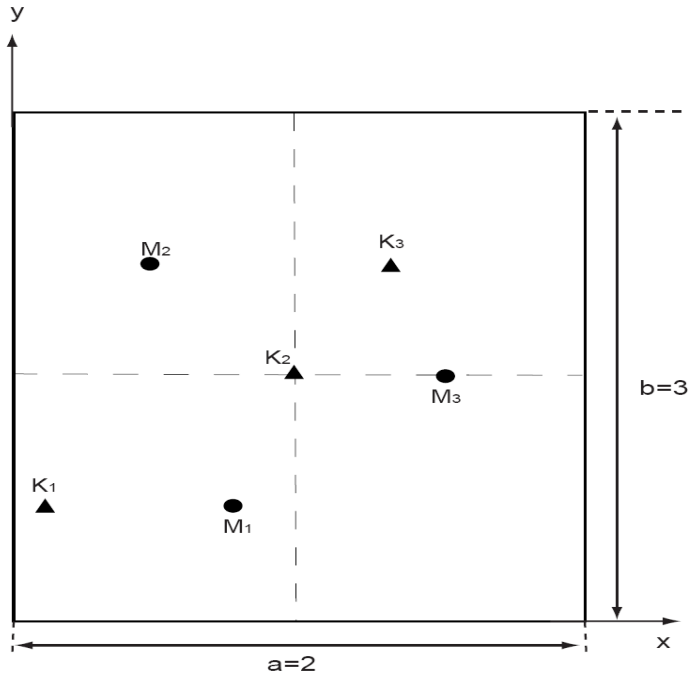

Figure 1: Schematic diagram of the plate with three concentrated masses (solid round dots) and three concentrated springs (solid triangle dots) in the computation example.

Because there are three concentrated masses and three concentrated springs (i.e. $r + s = 6$), matrix C is a 6×6 matrix. Newton-Raphson method is used to solve the characteristic equation of $|C| = 0$ to find the eigenfrequencies [18]. The first 6 lowest eigenfrequencies by FSTM are given in table 1 in comparison with those of Wu and Luo obtained by FEM and ANCM [10].

Table 1. Comparison of the eigenfrequencies (with the unit of Hertz) computed by FEM, ANCM and FSTM, respectively.

Methods/Eigenfrequency	ω_1	ω_2	ω_3	ω_4	ω_5	ω_6
FEM (ref. [10])	28.83	39.775	47.158	82.898	105.352	NA
ANCM (ref. [10])	28.632	39.392	48.084	81.836	104.038	NA
FSTM (this paper)	27.564	39.767	50.057	84.813	95.414	103.164

The first four lowest eigenfrequencies obtained by FSTM agree well with those obtained by both FEM and ANCM. However, ω_5 differs significantly. But it is worth noticing that ω_6 of FSTM is very close to ω_5 of FEM and ANCM (ω_6 values are not available in [10]). When Newton-Raphson method is applied to solve the eigenvalue problem of $|C| = 0$, the upper and lower bounds of each eigenfrequency must be carefully chosen before starting the computation [18]. Otherwise, Newton-Raphson method may miss the eigenfrequency but find another one.

4. CONCLUDING REMARKS

A generalized FSTM on the eignfrequency computation is presented and compared with other methods. For the eigenfrequency computation of a rectangular plate with four edges simply supported and 6 concentrated masses and springs, Wu and Luo's FEM is to solve an 175 × 175 matrix eigenvalue problem (175 is the element number)and ANCM is to solve a 30 × 30 matrix eigenvalue problem (30 is the mode number) [10]. In FSTM, 30 modes are also used to generate the elements of a 6×6 matrix of *C*. FSTM here essentially is to solve an eigenvalue problem of a 6×6 matrix determinant. When the plate does not have large number of concentrated masses and springs, FSTM is a much faster method to compute the eigenfrequencies. There is relatively small difference in the first four eigenfrequencies computed by FSTM, FEM and ANCM.

5. ACKNOWLEDGEMENTS

This work is supported by both the National Natural Science Foundation of China (NSFC, Grant No.10502050) and the Scientific Research Foundation for the Returned Overseas Chinese Scholars, State Education Ministry.

REFERENCES

[1] S. W. Wenzel and R. M. White, "Analytical comparison of the sensitivities of bulk-wave, surface-wave, and flexural plate-wave ultrasonic gravimetric sensors", *Applied Physics Letters* **54**, 1976-1978 (1989).

[2] B. Cunningham, M. Weinberg, J. Pepper, C. Clapp, R. Bousquet, B. Hugh, R. Kant, C. Daly and E. Hauser, "Design, fabrication and vapor characterization of a micrcofabricated flexural plate resonator sensor and application to integrated sensor arrays", *Sensors and Actuators B* **73**, 112-123 (2001).

[3] S. Dohn, R. Sandberg, W. Svendsen and A. Boisen, "Enhanced functionality of cantilever based mass sensors using higher modes" *Applied Physics Letters* **86**, 233501 (2005).

[4] T. Ono and M. Esashi, "Stress-induced mass detection with a

micromechanical/nanomechanical silicon resonator", *Review of Scientific Instruments* **76**, 093107 (2005).

[5] K. L. Ekinci, X. M. H. Huang and M. L. Roukes, "Ultrasensitive nanoelectromechanical mass detection", *Applied Physics Letters* **84**, 4469 (2004).

[6] B. Ilic, H. G. Craighead, S. Krylov, W. Senaratne, C. Ober and P. Neuzil, "Attogram detection using nanoelectromechanical oscillators", *Journal of Applied Physics* **95**, 3694 (2004).

[7] J. W. Grate, S. W. Wenzel and R. M. White, "Flexural plate wave devices for chemical analysis", *Analytical Chemistry* **63**, 1552-1561 (1991).

[8] E. T. Zellers, S. A. Batterman, M. Han and S. J. Patrash, "Optimal coating selection for the analysis of organic vapor mixtures with polymer-coated surface acoustic wave sensor arrays", *Analytical Chemistry* **67**, 1092-1106 (1995).

[9] Y. C. Das and D. R. Navaratna, "Vibrations of a rectangular plate with concentrated mass, spring, and dashpot", *Journal of Applied Mechanics* **30**, 31-36 (1963).

[10] J. S. Wu and S. S. Luo, "Use of the analytical and- numerical combined method in the free vibration analysis of a rectangular plate with any number of point masses and translational springs", *Journal of Sound and Vibration* **200**, 179-194 (1997).

[11] L. A. Bergman, J. K. Hall, G. G. G. Lueschen and D. M. McFarland, "Dynamic Green's function for Levy plates", *Journal of Sound and Vibration* **162,** 281-310 (1993).

[12] C. L. Amba-Rao, "On the vibration of a rectangular plate carrying a concentrated mass", *Journal of Applied Mechanics* **31**, 550-551 (1963).

[13] E. B. Magrab,"Vibration of a rectangular plate carrying a concentrated mass", *Journal of Applied Mechanics* **35**, 411-412 (1968).

[14] A. H. Shah and S. K. Datta, "Normal vibration of a rectangular plate with attached masses", *Journal of Applied Mechanics* **36**, 130-132 (1969).

[15] M. Chiba and T. Sugimoto, "Vibration characteristics of a cantilever plate with attached spring-mass system", *Journal of Sound and Vibration* **260**, 237-263 (2003).

[16] D. Ramos, J. Tamayo, J. Mertens, M. Calleja and A. Zaballos, "Origin of the response of nanomechanical resonators to bacteria adsorption," *Journal of Applied Physics*, **100,** 106105 (2006).

[17] D. J. Gorman 1982 *Free Vibration Analysis of Rectangular Plates*. New York: Elsevier North Holland.

[18] W. H. Press, B. P. Flannery, S. A. Teukolsky and W. T. Vettering 1986 *Numerical Recipes*. Cambridge University Press, Cambridge.